Journal of Solid State Chemistry **168,** 217–223 (2002)
doi:10.1006/jssc.2002.9713

Structures and Magnetic Properties of New Inserted Uranium Tellurides: $U_3Te_5Z_x$ (Z = Ge, Sn)

Olivier Tougait,[1] Michel Potel, and Henri Noël

Laboratoire de Chimie du Solide et Inorganique Moléculaire, Institut de Chimie, UMR 6511 CNRS, Université de Rennes1, Avenue du Général Leclerc, F-35042 Rennes, France

Received April 4, 2002; in revised form July 8, 2002; accepted July 16, 2002

The two new compounds $U_3Te_5Ge_{0.7}$ and $U_3Te_5Sn_{0.5}$ were prepared by heating the binary compound U_3Te_5 and the corresponding group 14 element at 850°C in a fused-silica tube. Single crystals have been grown by chemical vapor transport using iodine as transporting agent in temperature gradients of 870–840°C and 840–800°C for $U_3Te_5Ge_{0.7}$ and $U_3Te_5Sn_{0.5}$, respectively. They have been characterized by single-crystal X-ray diffraction measurements and by energy dispersive X-ray analysis. The two isostructural compounds crystallize with two formula units in the orthorhombic space group *Pmmn* in cells of dimensions: $U_3Te_5Ge_{0.7}$ $a = 4.2764(1)$ Å, $b = 13.1029(3)$ Å, $c = 8.9104(2)$ Å; $U_3Te_5Sn_{0.5}$, $a = 4.3160(1)$ Å, $b = 13.1999(4)$ Å, $c = 8.9128(2)$ Å. The crystal structures comprise two independent U atoms with two different coordination geometries. Atom U(1) is surrounded by eight Te atoms in a bicapped trigonal prismatic geometry. Atom U(2) is in a seven coordinate environment of Te atoms, with an arrangement usually described as a 7-octahedron. The three-dimensional packing results in distorted hexagonal cavities where the metalloid atoms are inserted. Magnetic measurements reveal that both compounds $U_3Te_5Ge_{0.7}$ and $U_3Te_5Sn_{0.5}$ are hard ferromagnets with ordering temperature of 135 and 140 K, respectively. At low temperature, they display large magnetocrystalline anisotropy with origin on the domain wall pinning at the magnetic domain boundaries.

Key Words: **single crystal; x-ray diffraction; nonstoichiometric compound; ferromagnet; magnetocrystalline anisotropy.**

INTRODUCTION

Binary uranium chalcogenides (U_yQ_z) have been widely studied because of their unusual structural, physical and electronic properties. Often, these materials show high temperature of magnetic ordering, large magnetocrystalline anisotropy, and mixed or intermediate valence character. Historically, the tellurides have received less attention than the sulfides or selenides. The more covalent nature of tellurium and its propensity to form a wide range of Te–Te interactions usually afford compounds with structures and properties that are significantly distinct from the sulfides and selenides. Therefore, there are stoichiometries such as UTe_5 (1, 2) and U_7Te_{12} (3) observed with tellurium that have not been found with sulfur and selenium. Moreover, according to the nature of the chalcogen (Q), binary phases can crystallize with different structure-types for a same stoichiometry. U_3Q_5 is known for Q = S, Se, Te. U_3S_5 and U_3Se_5 are isostructural compounds crystallizing with the U_3Se_5 structure-type (4, 5) whereas U_3Te_5 possesses a different structure-type (6).

In U_3Te_5, the three independent U atoms per unit-cell are surrounded by eight Te atoms in a bicapped trigonal prismatic geometry. Each independent UTe8 unit packs by edge-sharing to form a large hexacapped triprism having a trigonal prismatic cavity of six Te atoms located on its center. The crystal structure of U_3Te_5 consists of a three-dimensional arrangement of these large triprisms. They share their triangular faces along the shortest axis and join by sharing two edges to form infinite zig-zag chains running in the perpendicular plane. The formal oxidation state of the U cations cannot be readily assigned. The close examination of both the interatomic distances and magnetic structure (7) rather suggests an intermediate valence state for the three independent U cations.

The crystal structure of U_3Te_5 is closely related to that of YCo_5P_3 (8) which shows a similar network of trigonal prisms. In YCo_5P_3, the framework results from the packing of trigonal prisms of Co centered by P atoms. The main difference between the two structures is that the vacant prismatic site in U_3Te_5 is occupied by Y atoms in the ternary phosphide.

Following our constant interest on the solid-state compounds of uranium chalcogenides, subsequent syntheses were carried out to complete our observations about

[1] To whom correspondence should be addressed. Fax: ++33-2-99-38-34-87. E-mail: tougait@univ-rennes1.fr.

0022-4596/02 $35.00

the crystal chemistry of U_3Te_5. Considering the above-mentioned structural relationships, it was attempted to insert small cations in the framework of U_3Te_5. This series of experiments afforded the new compounds $U_3Te_5Ge_{0.7}$ and $U_3Te_5Sn_{0.5}$. The present article describes their syntheses, structures and magnetic properties.

EXPERIMENTAL

Syntheses

Pure powder of the binary compound U_3Te_5 was prepared as previously described in Ref. (6). Powder samples with composition of $U_3Te_5Ge_x$, where $x = 0.5, 0.7$ and 1, and $U_3Te_5Sn_x$, where $x = 0.5$ and 1, were prepared from the reaction of powders of the corresponding metalloid element and U_3Te_5 mixed in stoichiometric ratios. Cold-pressed pellets of the starting materials (ca. 0.5 g) were loaded into fused-silica tubes, which were then evacuated, sealed and heated at 850°C for 2 days. The products were analyzed by X-ray diffraction patterns collected on an Inel CPS 120 powder diffractometer with the use of a monchromatized Cu$K\alpha_1$ radiation. Depending on the ratio U_3Te_5:Z, very low-intensity reflections of either Ge and βSn elements or of the binary compound U_3Te_5 were observed, indicating a small amount of unreacted products. For both $U_3Te_5Ge_{0.7}$ and $U_3Te_5Sn_{0.5}$ syntheses, the ternary compounds were the major products. Single crystals were then grown from these bulk-phase samples by chemical vapor transport using iodine as transporting agent in temperature gradients of 870–840°C and 840–800°C for $U_3Te_5Ge_{0.7}$ and $U_3Te_5Sn_{0.5}$, respectively. Black, shiny single crystals with prismatic shape of $U_3Te_5Z_x$ (Z = Ge, Sn) as well as minor amounts of single crystals of UOTe were found in the cooler zone of the reaction tubes. Single crystals of UOTe having a characteristic triangular plate habitus could be easily distinguished from crystals of the target compounds. The origin of the contamination by oxygen may be ascribed to the chemical reaction of oxygen physically adsorbed on the starting materials as well as on the wall of the silica tubes. No transportation of the metalloids or U_3Te_5 was observed.

Single crystals of $U_3Te_5Ge_{0.7}$ and $U_3Te_5Sn_{0.5}$ were manually selected, washed with ethanol in order to remove all traces of iodine and finally dried with acetone.

Energy-Dispersive X-Ray (EDX) Analysis

EDX analyses were carried out with the use of a 6400JSM scanning electron microscope equipped with an Oxford Link Isis spectrometer. The presence of the three elements, U, Te and Z (Z = Ge, Sn) was systematically detected, but precise quantitative analysis could not be obtained as it requires proper external standards to superimpose to the internal ZAF corrections. However, the EDX results on Z (Z = Ge, Sn), relative to uranium and tellurium were constant and reproducible over several different single crystals from each preparation.

Crystal Structure Determination

Intensity data were collected on a Nonius Kappa CCD Diffractometer using a monochromatized Mo$K\alpha$ radiation ($\lambda = 0.71073$ Å) at room temperature. The frames were recorded using different ϕ ($\kappa = 0$) and ω scans with κ offset to fill more than half of the Ewald sphere. The exposure time per frame was of 153 and 60 s for $U_3Te_5Ge_{0.7}$ and $U_3Te_5Sn_{0.5}$, respectively. Data reduction and reflection indexing were performed with the use of the program DENZO of the Kappa CCD software package (9). For $U_3Te_5Ge_{0.7}$, the scaling and merging of redundant measurements of the different data sets as well as the global refinement of the crystal parameters were performed by SCALEPACK (9). For $U_3Te_5Sn_{0.5}$, the cell refinement was performed using DENZO, and a face-indexed absorption correction was made with the use of the program ANALYTICAL (10). Details on the crystallographic data are summarized in Table 1.

Systematic extinctions ($hk0$): $h + k = 2n + 1$, ($h00$): $h = 2n + 1$, ($0k0$): $k = 2n + 1$ led to the possible space groups $Pm2_1n$ and $Pmmn$. The structure was solved in the centrosymmetric space group by direct methods using SHELXS-97 (11). All structure refinements and Fourier syntheses were carried out using SHELXL-97 (11). Full-matrix least-squares refinements on F^2 of a model based on two U, three Te and one Z (Z = Ge, Sn) converged to residual values of $R(F) = 0.0607$ and 0.0711 for $U_3Te_5Ge_{0.7}$ and $U_3Te_5Sn_{0.5}$, respectively. For both structures, large negative residual electron densities were observed close to the position of the Z element. Moreover, their isotropic atomic displacements were about five times higher than those of the other atoms. Therefore the occupancy of Z was allowed to vary in subsequent structure refinements. Final refinements including a secondary extinction and anisotropic atomic displacement parameters for all atoms lowered the $R(F)$ values for reflections with $F_0^2 > 2\sigma(F_0^2)$ to 0.0354 and 0.0346 for $U_3Te_5Ge_{0.7}$ and $U_3Te_5Sn_{0.5}$, respectively. Refinements of the occupancy factors for the metalloid positions yielded to 0.725(4) and 0.463(3) values for Ge and Sn, respectively. Atomic coordinates and equivalent atomic displacement parameters, with their standard deviations, are given in Tables 2 and 3.

For both phases $U_3Te_5Ge_{0.7}$ and $U_3Te_5Sn_{0.5}$, a good agreement is observed between the composition that have been loaded in the reaction tubes and the formula deduced from the refinements on single crystal.

TABLE 1
Crystal Data and Structure Refinement for $U_3Te_5Ge_{0.7}$ and $U_3Te_5Sn_{0.5}$

Empirical formula	$U_3Te_5Ge_{0.7}$	$U_3Te_5Sn_{0.5}$
Formula weight	1402.82	1411.35
Crystal system, space group	Orthorhombic, *Pmmn* (no. 59)	
Unit-cell dimensions (Å)	$a = 4.2764(1)$	$a = 4.3160(1)$
	$b = 13.1029(3)$	$b = 13.1999(4)$
	$c = 8.9104(2)$	$c = 8.9128(2)$
Volume (Å^3)	499.28(2)	507.77(2)
Z, Calculated density (g/cm^3)	2, 9.33	2, 9.23
Absorption coefficient (cm^{-1})	657.3	641.3
Crystal color and habit	Black, prism	Black, rod
Crystal size (mm^3)	$0.08 \times 0.06 \times 0.05$	0.08×0.03-$\times 0.02$
Theta range for data collection (°)	2.29–45.28	2.28–37.02
Limiting indices	$-8 \le h \le 8$	$-7 \le h \le 7$
	$-24 \le k \le 26$	$-19 \le k \le 22$
	$-15 \le l \le 17$	$-13 \le l \le 15$
Reflections collected/unique	9256/2331	11247/1473
R(int)	0.0830	0.1026
Absorption correction	Scale-pack	Analytical
Max./min. transmission	None	0.055/0.295
Data/restraints/parameters	2331/0/33	1473/0/33
Goodness-of-fit on F^2	1.356	1.022
R indices[a] $[I > 2\sigma(I)]$	$R(F) = 0.0354$, $wR_2 = 0.0960$	$R(F) = 0.0346$, $wR_2 = 0.0755$
Extinction coefficient	0.0129(5)	0.0025(2)
Largest diff. peak and hole (e Å^{-3})	4.436 and −3.677	3.812 and −4.641

[a] $R(F) = \sum||F_o| - |F_c||/|F_c|$.

$wR_2 = [\sum w(F_o^2 - F_c^2)^2/wF_o^4]^{1/2}$, where $w^{-1} = \sigma^2(F_o^2) + (nF_o^2)^2$ for $F_o^2 \ge 0$ and $w^{-1} = \sigma^2(F_o^2)$ for $F_o^2 < 0$; $n = 0.045$ for $U_3Te_5Ge_{0.7}$ and $n = 0.04$ for $U_3Te_5Sn_{0.5}$.

Magnetic Measurements

Magnetic measurements for powder samples of $U_3Te_5Ge_{0.7}$ and $U_3Te_5Sn_{0.5}$ were made on a SQUID magnetometer (SHE- VTS) between 5 and 300 K. The zero-field cooled (ZFC) curves were obtained by cooling the samples from room temperature to 5 K in zero applied field and then measuring the magnetization with increasing the temperature in a certain field. The field cooled (FC) curves were obtained by cooling the samples from room temperature and then measuring magnetization with increasing the temperature in the same applied field as for the ZFC process. The applied fields were 2 and 5 kG for $U_3Te_5Ge_{0.7}$ and $U_3Te_5Sn_{0.5}$, respectively. For both compounds, the magnetization versus magnetic field measurements up to 30 kG were collected at 5 K. All magnetic data were corrected for sample holder.

TABLE 2
Atomic Coordinates and Equivalent Isotropic Displacement Parameters (Å^2) for $U_3Te_5Ge_{0.7}$

	Wyckoff position	Site occupancy	x	y	z	U_{eq}
U(1)	4*e*	1	$\frac{1}{4}$	0.5834(1)	0.2565(1)	0.015(1)
U(2)	2*a*	1	$\frac{1}{4}$	$\frac{1}{4}$	0.2789(1)	0.015(1)
Te(1)	4*e*	1	$\frac{1}{4}$	0.1020(1)	0.0084(1)	0.016(1)
Te(2)	4*e*	1	$\frac{1}{4}$	0.5830(1)	0.6264(1)	0.014(1)
Te(3)	2*a*	1	$\frac{1}{4}$	$\frac{1}{4}$	0.6379(1)	0.014(1)
Ge(1)	2*b*	0.725(4)	$\frac{1}{4}$	$\frac{3}{4}$	0.9912(1)	0.015(1)

U_{eq} is defined as one-third of the trace of the orthogonalized U_{ij} tensor.

TABLE 3
Atomic Coordinates and Equivalent Isotropic Displacement Parameters (Å^2) for $U_3Te_5Sn_{0.5}$

	Wyckoff position	Site occupancy	x	y	z	U_{eq}
U(1)	4*e*	1	$\frac{1}{4}$	0.5801(1)	0.2560(1)	0.012(1)
U(2)	2*a*	1	$\frac{1}{4}$	$\frac{1}{4}$	0.2858(1)	0.013(1)
Te(1)	4*e*	1	$\frac{1}{4}$	0.1031(1)	0.0109(1)	0.018(1)
Te(2)	4*e*	1	$\frac{1}{4}$	0.5838(1)	0.6247(1)	0.012(1)
Te(3)	2*a*	1	$\frac{1}{4}$	$\frac{1}{4}$	0.6441(1)	0.012(1)
Sn(1)	2*b*	0.463(3)	$\frac{1}{4}$	$\frac{3}{4}$	0.9885(2)	0.011(1)

U_{eq} is defined as one-third of the trace of the orthogonalized U_{ij} tensor.

RESULTS AND DISCUSSION

Structural Description

The compounds $U_3Te_5Ge_{0.7}$ and $U_3Te_5Sn_{0.5}$ adopt a novel structure-type. Selected interatomic distances for both compounds are given in Table 4. A perspective view of the structure of $U_3Te_5Sn_{0.5}$ is displayed in Fig. 1. Atom

TABLE 4
Selected Interatomic Distances (Å) for $U_3Te_5Ge_{0.7}$ and $U_3Te_5Sn_{0.5}$

	$U_3Te_5Ge_{0.7}$	$U_3Te_5Sn_{0.5}$
U(1)–Te(1) × 2	3.194(1)	3.226(1)
U(1)–Te(3) × 2	3.197(1)	3.238(1)
U(1)–Te(2) × 2	3.227(1)	3.235(1)
U(1)–Te(1)	3.284(1)	3.259(1)
U(1)–Te(2)	3.296(1)	3.286(1)
U(1)–*Z*	3.217(1)	3.274(2)
U(2)–Te(1) × 2	3.093(1)	3.124(1)
U(2)–Te(2) × 4	3.174(1)	3.179(1)
U(2)–Te(3)	3.199(1)	3.194(1)
U(2)–*Z* × 2	3.220(1)	3.261(2)
Z–Te(1) × 4	2.887(1)	2.901(1)
Z–U(1) × 2	3.217(1)	3.274(2)
Z–U(2) × 2	3.220(1)	3.261(2)
Z–*Z* × 2	4.2764(1)	4.3160(1)

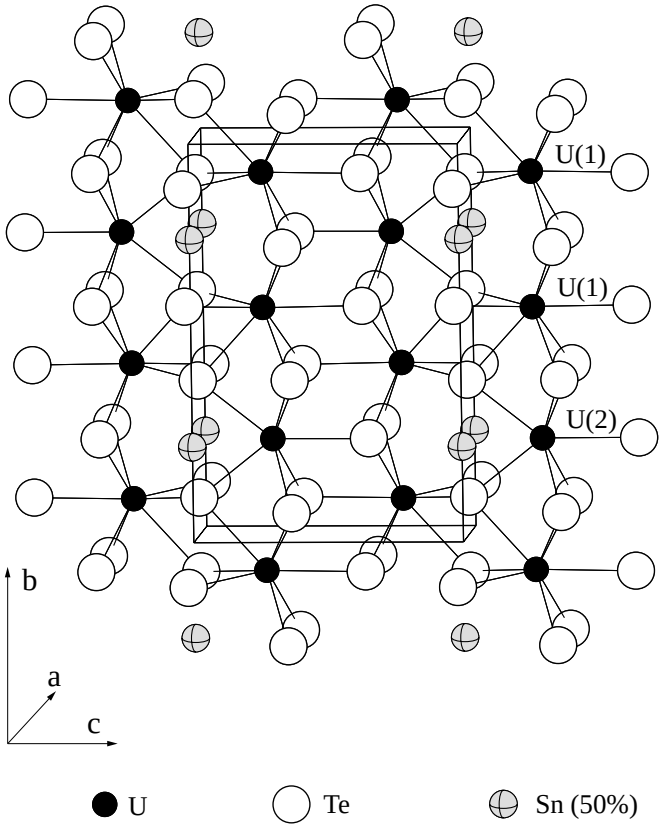

FIG. 1. Perspective view of the unit-cell of $U_3Te_5Sn_{0.5}$ down *a*-axis.

U(1) is surrounded by eight Te atoms in a bicapped trigonal prismatic geometry. Atom U(2) is in a seven-coordinate environment of Te atoms, with four Te atoms in an equatorial plane and three other Te atoms in a perpendicular plane, an arrangement usually described as a 7-octahedron with one apex split into two positions.

The main building units of the structure are motifs derived from trigonal prisms and octahedra. The height of these moieties corresponds to the length of the shortest axis (*a*-axis), and thus the interconnection in the [100] direction occurs by face sharing of trigonal prisms and Te–Te edge sharing of 7-octahedra. The structure of $U_3Te_5Z_x$ compounds can be viewed as a succession along the *b*-axis of chains constructed from two adjacent U(1)Te8 bicapped trigonal prisms separated by a single polyhedron centered by U(2). Within the chains, U(2)Te7 units share triangular faces with their two U(1)Te8 near neighbors, whereas U(1)Te8 motifs are joined by edge sharing. Figure 2 displays a perspective view along the *a*-axis of the packing within the strand, as well as the labeling scheme. Along the *c*-direction, the resulting chains are alternatively connected in a rock-salt fashion and by sharing a common Te atom between two U(1)Te8 bicapped trigonal prisms and one U(2)Te7 7-octahedron. The junction thus constituted also defines distorted hexagonal cavities where the metalloid atoms are inserted.

The three-dimensional structure of $U_3Te_5Z_x$ (Z = Ge, Sn) compounds results in unusual coordination geometry about the Z atoms (Fig. 3). They are surrounded by four U atoms in a tetrahedral geometry and four Te atoms in a square-planar fashion. For each compound, the $Z-Z$ separation corresponds to the *a* parameter (see Table 4) which is far above any electronic interactions. Examination of reported Ge (12–15) or Sn (16–18) ternary telluride compounds rather suggests small coordination numbers about Ge or Sn, usually three or four, with bonding distances in the vicinity of 2.60 and 2.80 Å for Ge and Sn, respectively. The square-planar environment of Te atoms

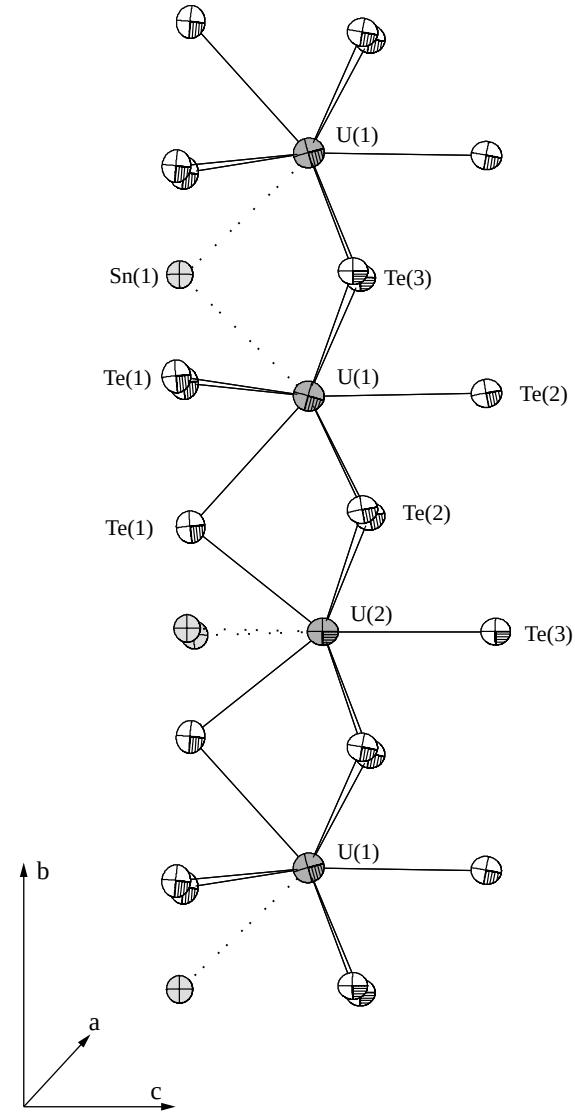

FIG. 2. Perspective view down *a*-axis of the packing of the uranium polyhedra within the chain. Ellipsoids are drawn at the 90% probability level.

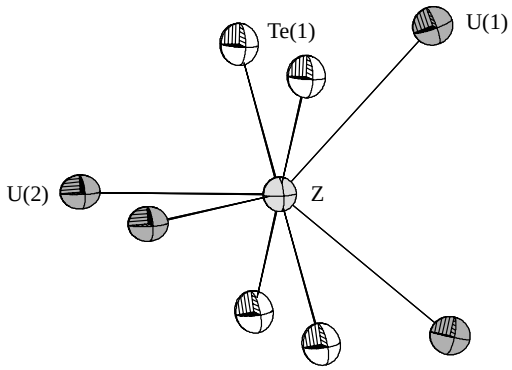

FIG. 3. View of the environment of the metalloid atoms found in $U_3Te_5Z_x$ (Z = Ge, Sn). Ellipsoids are drawn at the 90% probability level.

about Ge and Sn is not abnormal; it has also been observed in the ternary compounds Tl_2GeTe_5 (13) and Tl_2SnTe_5 (17) and in the intercalated compound $NbGe_{0.5}Te_2$ (15). The Ge–Te distances of 2.887(1) Å in $U_3Te_5Ge_{0.7}$ are significantly longer than those in these reported compounds. On the opposite, the Sn–Te distances in $U_3Te_5Sn_{0.5}$ are slightly longer than the average value given above. The value of 2.901(1) Å is reasonable for bonding.

The U–Z distances are also an interesting feature in $U_3Te_5Z_x$ (Z = Ge, Sn) compounds. Unlike the U–Sn distances of 3.274(2) and 3.261(2) Å which compare well those found in binary uranium stannides (19) or ternary alloys such as UFe_5Sn (20) (3.230–3.273 Å), the U–Ge distances of 3.217(1) and 3.220(1) Å in $U_3Te_5Ge_{0.7}$ are much longer than an average value for bonding of 3.05 Å deduced from the literature on uranium germanides (21–25). It must be thus emphasized that the spacing between Sn and its first coordination sphere compares reasonably well bonding distances whereas in the Ge counterpart, the same spacing appears too long for usual distances of bonds.

For both compounds $U_3Te_5Ge_{0.7}$ and $U_3Te_5Sn_{0.5}$, the U–Te distances atoms are close to those reported for the binary uranium tellurides U_3Te_5 (6) and U_2Te_3 (26). Similar to these two binary compounds, the formal oxidation state of the two crystallographically independent U cations of $U_3Te_5Ge_{0.7}$ and $U_3Te_5Sn_{0.5}$ compounds cannot be unambiguously deduced from the values of the mean interatomic distances.

Nonstoichiometry of Z

Regarding the nonstoichiometry of the metalloids in the U_3Te_5 framework, Ge and Sn behave quite distinctly. X-rays diffraction analyses on single crystals of $U_3Te_5Ge_x$ found in a series of reactions in which the content of Ge (x) was allow to vary, give values of x ranging from 0.7 to 1. When the crystallographic site of the Ge position is fulfilled, reconstruction of precession images shows weak supplementary reflections which could be indexed by doubling the c-axis. However, refinement of the crystal structure in this double unit-cell did not lead to satisfactory residual and atomic parameters. Re-examination of the newly indexed reflections shows at high θ angle an increase of the difference between the observed and the calculated positions of the reflections with odd l indices, rather suggesting a modulated structure with a propagation vector $\mathbf{q}$ close to $\frac{1}{2}c^*$. A similar observation that a variation of the amount of cations inserted in an U–Te framework induces a subtle evolution of the structure has been already proposed for the series of compounds Cu_xUTe_3 (27, 28). In this latter case, the intercalation of copper between UTe_3 layers directly impacts on the Te network and induces structural modifications.

Unlike for the Ge-containing analogue. The X-ray diffraction analyses undertaken on single crystals of $U_3Te_5Sn_x$ synthesized with various starting contents of Sn (x = 0.5, 1) yield to a reproducible value of x close to 0.5. Moreover, reconstruction of precession images along the three axes did not show any supplementary reflections other than that corresponding to the orthorhombic P type-lattice with cell parameters gathered in Table 1.

Magnetic Properties

The isothermal magnetization versus magnetic field (Fig. 4) and the temperature dependence of the magnetization (Fig. 5) reveal that $U_3Te_5Z_x$ (Z = Ge, Sn) compounds are hard ferromagnetic materials with large magnetocrystalline anisotropy at low temperature. For both compounds $U_3Te_5Ge_{0.7}$ and $U_3Te_5Sn_{0.5}$ the ferromagnetic parameters such as Curie temperature (T_C), spontaneous

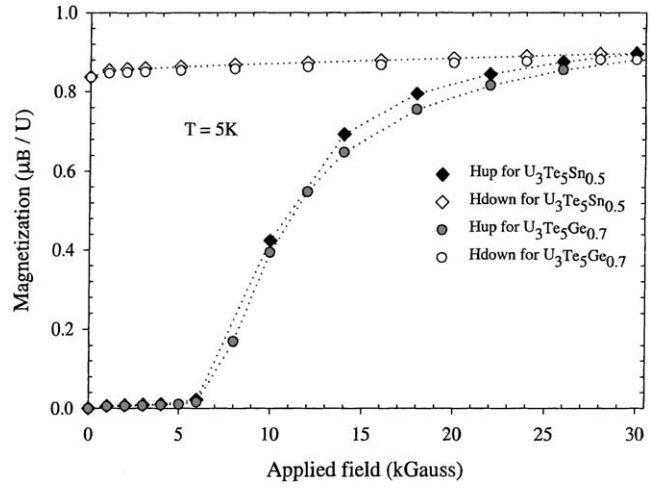

FIG. 4. Magnetization versus magnetic field for $U_3Te_5Ge_{0.7}$ and $U_3Te_5Sn_{0.5}$ at 5 K.

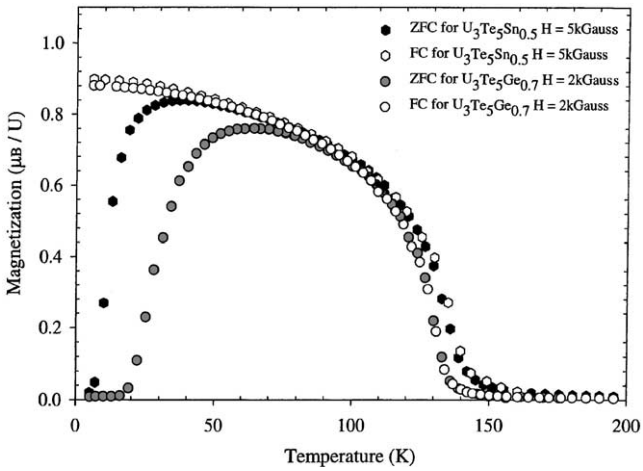

FIG. 5. Temperature dependence of the magnetization for $U_3Te_5Ge_{0.7}$ and $U_3Te_5Sn_{0.5}$ after ZFC or FC.

magnetization (M_s) and coercive field as well as the paramagnetic parameters are very similar (see Table 5).

The isothermal magnetization curves (Fig. 4) which correspond to the initial magnetization reveal large magnetocrystalline anisotropy. The reversible boundary displacements occur up to 6 kG which corresponds to the coercive field. It is well known that narrow domain wall pinning takes place on obstacles of atomic scale for which the magnetic moments are opposed to the direction of the easy magnetization. The phenomenon vanishes either when a sufficient field is applied or when a certain temperature is reached. The irreversible behaviors observed on the ZFC–FC curves (Fig. 5), are also featuring the magnetocrystalline anisotropy. Since $U_3Te_5Ge_{0.7}$ and $U_3Te_5Sn_{0.5}$ have the same value of the coercive field at $T = 5$ K, the freezing temperature at which the irreversibility occurs decrease with increasing field as illustrated on Fig. 5. The freezing temperature, deduced on the thermomagnetic curve of $U_3Te_5Ge_{0.7}$ measured at 2 kG is higher than that of $U_3Te_5Sn_{0.5}$ measured at 5 kG.

For the $U_3Te_5Z_x$ (Z = Ge, Sn) compounds, the magnetic saturation is not completely reached under 30 kG giving a magnetization value of $0.84(1)\,\mu_B$/U at 5 K. The Curie temperatures deduced form the temperature dependence of the magnetization curves are close to 135 and 140 K for $U_3Te_5Ge_{0.7}$ and $U_3Te_5Sn_{0.5}$, respectively. In the paramagnetic region, the magnetic susceptibilities versus temperature were fitted by a modified Curie–Weiss law leading to the values listed in Table 5. The effective magnetic moments are significantly lower than the calculated values assuming a Russel–Saunders coupling, U^{3+} ($3.62\,\mu_B$), U^{4+} ($3.58\,\mu_B$). However, such reduced values are commonly reported, with origin ascribed to the degree of delocalisation of the 5-f electrons and/or to crystal field effects (29). As a consequence, it is well believed that magnetic measurements are inappropriate tools to assign the valence state between U^{3+} and U^{4+} cations.

TABLE 5
Magnetic Parameters for $U_3Te_5Ge_{0.7}$ and $U_3Te_5Sn_{0.5}$

Compounds	T_C (K)	Ms (μ_B/U)	μ_{eff} (μ_B/U)	θ_p (K)	χ_o (emu/mol)
$U_3Te_5Ge_{0.7}$	135(3)	0.836(9)	2.25(2)	130(1)	$4.00\,E^{-3}$
$U_3Te_5Sn_{0.5}$	140(3)	0.837(9)	2.19(2)	137(1)	$3.10\,E^{-3}$

Since the insertion of metalloids in the U_3Te_5 framework induces dramatic structural changes, it indicates that strong electronic interactions may occur between the host structure and the incorporated element. However, the magnetic properties of $U_3Te_5Ge_{0.7}$ and $U_3Te_5Sn_{0.5}$, being almost identical, suggest that the overall electronic properties of the homologous series of compounds $U_3Te_5Z_x$ (Z = Ge, Sn) are weakly dependent of the nature and the amount of Z. In order to evaluate more deeply the corresponding electron transfer, further investigations are required: (i) insertion of other metalloids having intermediate electronegativity, such as Ga, As, Hg or Pb, (ii) complementary crystallographic characterizations including the modulation detected on the single crystal X-rays diffraction experiments of $U_3Te_5Ge_1$, and (iii) neutron diffraction studies of the magnetic structures. These subsequent experiments are currently under progress.

ACKNOWLEDGMENT

Use was made of the Nonius Kappa CCD diffractometer through the Centre de Diffraction X de l'Université de Rennes1 (CDIFX).

REFERENCES

1. H. Noël, *Mater. Res. Bull.* **19,** 1171 (1984).
2. H. Noël, *Inorg. Chim. Acta* **109,** 205 (1985).
3. O. Tougait, M. Potel, and H. Noël, *Inorg. Chem.* **139,** 5088 (1998).
4. M. Potel, R. Brochu, J. Padiou, and D. Grandjean, *C. R. Acad. Sci. Sér. C* **215,** 1419 (1972).
5. P. T. Moseley, D. Brown, and B. Wittaker, *Acta Crystallogr. Sect. B* **28,** 1816 (1972).
6. O. Tougait, M. Potel, and H. Noël, *J. Solid State Chem.* **139,** 356 (1998).
7. O. Tougait, G. André, F. Bourée, and H. Noël, *J. Alloys Compd.* **317/318,** 227 (2001).
8. U. Meisen and W. Jeitschko, *J. Less-Common Met.* **102,** 127 (1984).
9. Nonius, *in* "Collect, Denzo, Scalepack, Sortav," Kappa CCD Program Package. Nonius BV, Delft, The Netherlands, 1998.
10. J. de Meulenaar and H. Tompa, *Acta Crystallogr. Sect. A* **19,** 1014 (1965).
11. G. M. Sheldrick, Shelxs97 and Shelxl97, University of Göttingen, Germany.
12. B. Eisenmann, H. Schord, and H. Schäfer, *Mater. Res. Bull.* **19,** 293 (1984).

13. A. A. Touré, G. Kra, R. Eholié, J. Olivier-Fourcade, J. Jumas, and M. Maurin, *J. Solid State Chem.* **84,** 245 (1990).
14. A. Mar and J. A. Ibers, *J. Am. Chem. Soc.* **115,** 3227 (1993).
15. J. Gareh, F. Boucher, and M. Evain, *Eur. J. Solid State Inorg. Chem.* **33,** 355 (1996).
16. B. Eisenmann, H. Schwerer, and H. Schäfer, *Mater. Res. Bull.* **18,** 383 (1983).
17. V. Agafonov, B. Legendre, N. Rodier, J. M. Cense, E. Dichi, and G. Kra, *Acta Crystallogr. Sect. C* **47,** 850 (1991).
18. J. Li, Y. Y. Liszewski, L. A. MacAdams, F. Chen, S. Mulley, and D. M. Proserpio, *Chem. Mater.* **8,** 598 (1996).
19. A. Palenzona and P. Manfrinetti, *J. Alloys Compd.* **221,** 157 (1995).
20. A. P. Gonçalves, M. Godinho, and H. Noël, *J. Solid State Chem.* **154,** 551 (2000).
21. P. Boulet, A. Daoudi, M. Potel, H. Noël, G. M. Gross, G. André, and F. Bourée, *J. Alloys Compd.* **247,** 104 (1997).
22. P. Rogl, G. André, F. Weitzer, M. Potel, and H. Noël, *J. Solid State Chem.* **131,** 72 (1997).
23. P. Boulet, M. Potel, J. C. Levet, and H. Noël, *J. Alloys Compd.* **262/263,** 229 (1997).
24. P. Boulet, M. Potel, G. André, P. Rogl, and H. Noël, *J. Alloys Compd.* **283,** 41 (1999).
25. P. Boulet, G. M. Gross, G. André, F. Bourée, and H. Noël, *J. Solid State Chem.* **144,** 311 (1999).
26. O. Tougait, M. Potel, J. C. Levet, and H. Noël, *Eur. J. Solid State Inorg. Chem.* **35,** 67 (1998).
27. R. Patschke, J. D. Breshears, P. Brazis, C. R. Kannewurf, S. J. L. Billinge, and M. G. Kanatzidis, *J. Am. Chem. Soc.* **123,** 4755 (2001).
28. F. Q. Huang and J. A. Ibers, *J. Solid State Chem.* **159,** 186 (2001).
29. D. J. Lam and A. T. Aldred, *in* "The Actinides: Electronic Structure and Related Properties, Vol. 1, Materials Science Series" (A. J. Freeman and J. B. Darby Jr., (Eds.)), pp. 109–174. Academic Press, New York, 1974.